

## Aerosol anthropogenic component estimated from satellite data

Y. J. Kaufman,<sup>1</sup> O. Boucher,<sup>2,3</sup> D. Tanré,<sup>4</sup> M. Chin,<sup>1</sup> L. A. Remer,<sup>1</sup> and T. Takemura<sup>1,5</sup>

Received 31 March 2005; revised 5 July 2005; accepted 19 July 2005; published 3 September 2005.

[1] Satellite instruments do not measure the aerosol chemical composition needed to discriminate anthropogenic from natural aerosol components. However the ability of new satellite instruments to distinguish fine (submicron) from coarse (supermicron) aerosols over the oceans, serves as a signature of the anthropogenic component and can be used to estimate the fraction of anthropogenic aerosols with an uncertainty of  $\pm 30\%$ . Application to two years of global MODIS data shows that  $21 \pm 7\%$  of the aerosol optical thickness over the oceans has an anthropogenic origin. We found that three chemical transport models, used for global estimates of the aerosol forcing of climate, calculate a global average anthropogenic optical thickness over the ocean between 0.030 and 0.036, in line with the present MODIS assessment of 0.033. This increases our confidence in model assessments of the aerosol direct forcing of climate. The MODIS estimated aerosol forcing over cloud free oceans is therefore  $-1.4 \pm 0.4 \text{ W/m}^2$ .

**Citation:** Kaufman, Y. J., O. Boucher, D. Tanré, M. Chin, L. A. Remer, and T. Takemura (2005), Aerosol anthropogenic component estimated from satellite data, *Geophys. Res. Lett.*, 32, L17804, doi:10.1029/2005GL023125.

### 1. Introduction

[2] Climate change research [*Intergovernmental Panel on Climate Change (IPCC)*, 2001] and studies of the aerosol forcing on the hydrological cycle [*Ramanathan et al.*, 2001] require knowledge of the anthropogenic component of the aerosol. Natural aerosols can cause variability in the climate system and be part of its feedback mechanisms, e.g. larger amount of dust generated during drought conditions in the Sahel [*Prospero and Lamb*, 2003] can cause cooling of the earth system and changes in the drought conditions. Only anthropogenic aerosol can be considered as an external cause of climate change [*Charlson et al.*, 1992]. Aerosol exerts a radiative forcing of climate via direct absorption and reflection of sunlight to space and via induced changes in the cloud microphysics, water content, and coverage [*Gunn and Phillips*, 1957; *Twomey et al.*, 1984; *Albrecht*, 1989; *Rosenfeld*, 2000; *Koren et al.*, 2004].

[3] Yet assessments of the aerosol radiative forcing [*IPCC*, 2001] are based only on models since we do not have a

method to measure the amount and distribution of anthropogenic aerosol around the Earth. Previously [*Kaufman et al.*, 2002] we suggested that satellite data that distinguish fine from coarse aerosols can be used for this purpose. The reason is that natural and anthropogenic aerosols have different proportions of fine and coarse aerosols. Urban/industrial pollution and smoke from vegetation burning (mostly anthropogenic) have mostly fine aerosol, while dust and marine aerosols (mostly natural) are dominated by coarse aerosol but with significant fine aerosol fraction [*Tanré et al.*, 2001; *Kaufman et al.*, 2001].

[4] Here we use MODIS measurements over the oceans of the aerosol optical thickness and the fraction of the optical thickness contributed by fine aerosol [*Tanré et al.*, 1997; *Remer et al.*, 2005], to derive the anthropogenic optical thickness. The results are used to evaluate chemical transport models that are used to assess the aerosol forcing of climate.

### 2. Analysis

[5] The method for satellite based estimate of the aerosol anthropogenic component is based on the following assumptions:

[6] 1) The fraction of the aerosol optical thickness contributed by the fine aerosol is constant for a given aerosol type; e.g. fine aerosol dominates the optical properties for smoke and pollution and coarse aerosol dominates dust and maritime aerosol.

[7] 2) All smoke is from anthropogenic origin and all dust is natural. It is estimated that about 20% of biomass burning originates from wild fires [*Hobbs et al.*, 1997]. About 10% of the dust can be from anthropogenic sources [*Tegen et al.*, 2004]. We shall account for the smoke overestimate but not dust later in the paper.

[8] 3) MODIS derivation of the fine fraction is consistent: any errors in the derivation of the fine fraction are constant and the correlation with the true fine fraction is very good.

[9] 4) Based on AERONET and MODIS analysis [*Kaufman et al.*, 2001, 2005] it is assumed that the baseline marine aerosol optical thickness is  $0.06 \pm 0.01$ . This is the average marine optical thickness for calm conditions. Strong winds can elevate the sea salt concentration.

[10] We represent the total aerosol optical thickness  $\tau_{550}$  by its anthropogenic (air pollution and smoke aerosol) -  $\tau_{\text{anth}}$ , dust -  $\tau_{\text{dust}}$ , and baseline marine -  $\tau_{\text{mar}}$ , components:

$$\tau_{550} = \tau_{\text{anth}} + \tau_{\text{dust}} + \tau_{\text{mar}} \quad (1)$$

The fine aerosol optical thickness,  $\tau_f$ , measured by the satellite can be described as:

$$\tau_f = f_{550} \tau_{550} = f_{\text{anth}} \tau_{\text{anth}} + f_{\text{dust}} \tau_{\text{dust}} + f_{\text{mar}} \tau_{\text{mar}} \quad (2)$$

<sup>1</sup>NASA Goddard Space Flight Center, Greenbelt, Maryland, USA.

<sup>2</sup>Climate, Chemistry, and Ecosystems Team, Met Office, Exeter, UK.

<sup>3</sup>Formerly at Laboratoire d'Optique Atmosphérique, CNRS, Université des Sciences et Technologies de Lille 1, Villeneuve d'Ascq, France.

<sup>4</sup>Laboratoire d'Optique Atmosphérique, CNRS, Université des Sciences et Technologies de Lille 1, Villeneuve d'Ascq, France.

<sup>5</sup>Permanently at Research Institute for Applied Mechanics, Kyushu University, Fukuoka, Japan.

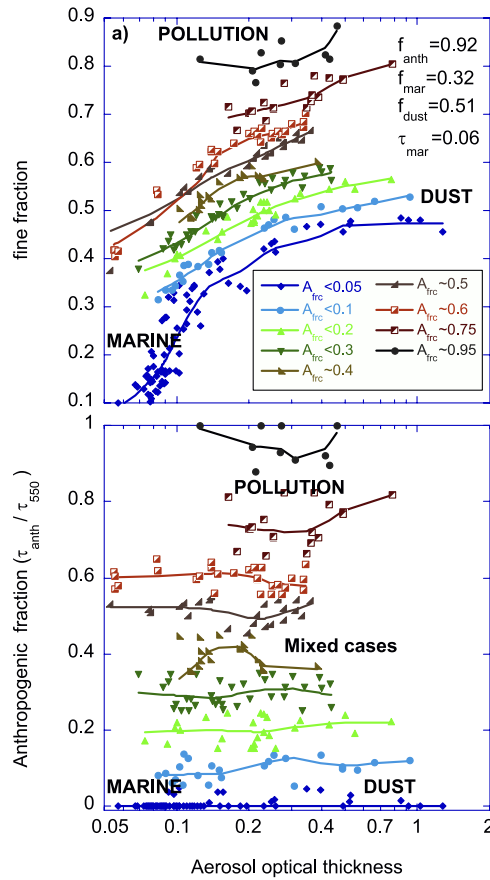


**Figure 1.** (a) Classification of the global aerosol over the oceans using MODIS data in coordinates of the optical thickness and the fine fraction. Colors - the derived fraction of the aerosol optical thickness from anthropogenic sources (equation (4),  $A_{frc} = \tau_{anth} / \tau_{550}$ ). Each point represents an average for the month of July 2002 for a  $10^\circ$  latitude and longitude grid box. (b) Same but for the anthropogenic fraction, showing the stratification of the aerosol measurements with the anthropogenic fraction.

Here we have 2 equations and 6 unknowns, 3 of them:  $f_{mar}$ ,  $f_{dust}$ ,  $f_{anth}$  – the marine, dust and anthropogenic fine fractions, are directly derived from MODIS over specific locations, one of them,  $\tau_{mar}$  – the marine aerosol optical thickness is determined from AERONET and the other two: the total fine fraction and optical thickness:  $f_{550}$  and  $\tau_{550}$  are derived by MODIS. Impact of uncertainties in these quantities is discussed in the next section. From equations (1) and (2),  $\tau_{dust}$  is extracted:

$$\tau_{dust} = [f_{550}\tau_{550} - f_{anth}\tau_{anth} - f_{mar}\tau_{mar}] / f_{dust} \quad (3)$$

Substituting  $\tau_{dust}$  from equation (3) into equation (1) we get the expression for  $\tau_{anth}$ :

$$\tau_{anth} = [(f_{550} - f_{dust})\tau_{550} - (f_{mar} - f_{dust})\tau_{mar}] / (f_{anth} - f_{dust}) \quad (4)$$

The values of  $f_{dust}$ ,  $f_{mar}$  and  $f_{anth}$  are determined using two-dimensional classification of the MODIS data, in  $f_{550} \times \tau_{550}$  coordinates (see Figure 1a).  $f_{mar}$  is determined in clean marine region ( $20^\circ - 30^\circ S$ ,  $50^\circ - 120^\circ E$ ), for the whole year of 2002, as  $f_{mar} = 0.32 \pm 0.07$ .  $f_{dust}$  is determined West of the African coast ( $15^\circ - 20^\circ W$ ,  $15^\circ N - 20^\circ N$ ) for June–October 2002 as  $f_{dust} = 0.51 \pm 0.03$ , and  $f_{anth}$  over the Wester Atlantic ( $40^\circ - 50^\circ N$ ,  $70^\circ - 90^\circ W$  for June and  $60^\circ - 80^\circ W$  for July) as  $f_{anth} = 0.92 \pm 0.03$ . In determination of  $f_{anth}$  and  $f_{dust}$  first the marine contribution was subtracted using equations (1)–(2). These values are then used to determine the anthropogenic optical thickness,  $\tau_{anth}$ , for each location and time using the MODIS daily measured  $\tau_{550}$  and  $f_{550}$  values. Figure 1b shows scatter plot of the anthropogenic fraction ( $A_{frc} = \tau_{anth} / \tau_{550}$ ) derived from equation (4), as a function of the aerosol optical thickness. It shows that the transformation of the coordinates from  $(f_{550}, \tau_{550})$  to  $(A_{frc}, \tau_{550})$  generates, as expected, a fixed anthropogenic fraction for the different aerosol types.

[11] Note that equation (4) is based on the baseline value of the clean marine aerosol optical thickness. In regions with stronger winds and higher sea salt concentration equation (4) attributes the extra coarse sea salt particles to

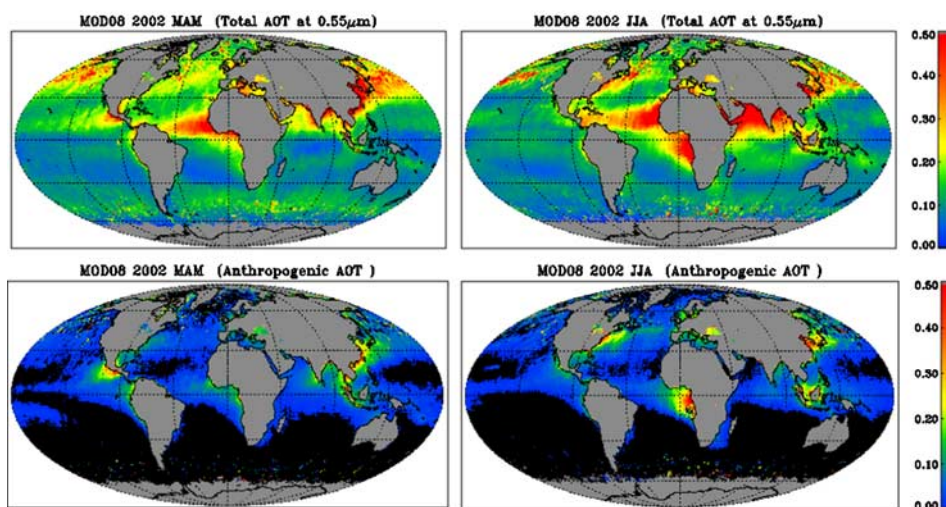


**Figure 2.** Global distribution over the oceans of (top) the total aerosol optical thickness and (bottom) the anthropogenic component derived from the MODIS data and equation (4): (left) March–May, (right) June–Aug., 2002.

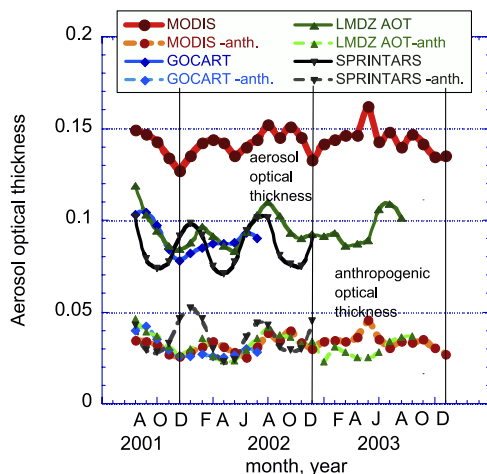


**Figure 3.** Global average aerosol optical thickness over cloud free ocean (top) measured by MODIS (red), and (middle) simulated by GOCART (blue), LMDZ (green) and SPRINTARS (black) models. Bottom: Anthropogenic aerosol optical thickness for MODIS (red) and models. MODIS mostly agrees with models regarding the anthropogenic component (averages of 0.033-MODIS, 0.032-LMDZ, 0.030-GOCART and 0.036-SPRINTARS).

dust, resulting in negative anthropogenic optical thickness in the process. In such cases the anthropogenic optical thickness is set to zero. Note also that values of the fine fraction, and mainly of marine aerosol are very sensitive to details of the algorithm and MODIS calibration and can change with time and algorithm version.

[12] Application of equation (4) to global data shows the distribution of the anthropogenic aerosol (Figure 2). Dust from Africa and East Asia, present in the maps of the total aerosol are absent from the maps of the anthropogenic component. High levels of anthropogenic aerosol are observed near Central America in March–May, North America in and South Africa in June–Aug and East Asia year round.

### 3. Comparison to Models

[13] Estimates of the aerosol forcing of climate are based on chemical transport models that describe the global aerosol evolution using detailed account of aerosol sources and processes in the atmosphere. To what degree the model predictions of the anthropogenic aerosol optical thickness fit the observations? Several papers reported comparison of the model total optical thickness to ground based and satellite measurements but not the anthropogenic component.

[14] Here we can test the following hypothesis: let us assume that models have a better account for anthropogenic sources (counting cars, fires and energy consumption) than of natural production of wind dependent sea salt and dust. We also know that MODIS has some residual contamination from very thin cirrus [Remer et al., 2005]. Since cloud contamination has similar spectral signature to coarse dust or sea salt particles, it contributes to errors in the MODIS derived coarse mode optical thickness but not the derived fine aerosol optical thickness. Therefore, the large difference in the total aerosol optical thickness between MODIS and models ( $\Delta\tau_{550} \sim 0.05$ ), shown in Figure 3 should not

be translated into large differences in the anthropogenic component.

[15] This hypothesis is tested in Figure 3 by comparing MODIS data with simulations of the SPRINTARS [Takemura et al., 2002], GOCART [Chin et al., 2002] and LMDZ (M. S. Reddy et al., Global multi-component aerosol optical depths and radiative forcing estimates in the LMDZT general circulation model, submitted to *Journal of Geophysical Research*, 2005) models. The models also assume that all smoke aerosol is anthropogenic and all dust is natural. Despite the large differences between models and MODIS for the total optical thickness, the MODIS anthropogenic optical thickness agrees well with the LMDZ and GOCART models and most of the time also with the SPRINTARS model, with average difference between MODIS and models of  $\Delta\tau_{\text{anth}} = 0.001$  to 0.006.

[16] Comparison between the MODIS and models latitudinal dependence of the global average aerosol optical thickness and anthropogenic component is shown in Figure 4. There is a very good agreement among them. Note that the increase in the optical thickness at  $40^{\circ}\text{S}$ – $60^{\circ}\text{S}$  due the strong wind driven sea salt is not translated, as expected, into an anthropogenic component. In the Southern Ocean,  $60$ – $80^{\circ}\text{S}$ , MODIS derives a larger anthropogenic optical thickness than the models. Enhanced DMS production in this region that is not accounted for by the algorithm can be the reason.

[17] The global average anthropogenic fraction, defined as ratio between the anthropogenic optical thickness and the total optical thickness, is for MODIS 0.23 for the data in Figure 3 and 0.33 to 0.42 for the models. We performed sensitivity study to uncertainties in the fine fraction of dust ( $\Delta f_{\text{dust}} = \pm 0.03$ ), maritime aerosol fine fraction ( $\Delta f_{\text{mar}} = \pm 0.07$ ), pollution and smoke fine fraction ( $\Delta f_{\text{anth}} = \pm 0.03$ ) and in the maritime baseline value of aerosol optical thickness ( $\pm 0.01$ ). The results show uncertainty in the global

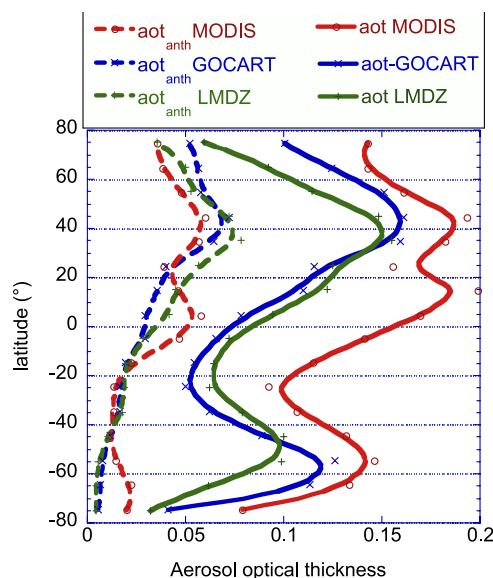


**Figure 4.** Latitude dependence of the total (solid lines) and the anthropogenic (dashed lines) aerosol optical thickness for MODIS (red), LMDZ (green) and GOCART (blue) models. The MODIS and LMDZ data are for 2002 and the GOCART data for Aug 2001–July 2002.

average anthropogenic fraction of  $\pm 0.06$  or in the anthropogenic optical thickness of  $\Delta\tau_{\text{anth}} = \pm 0.01$ . Accounting for the fact that 80% not 100% of the biomass burning is in the tropics [Hobbs *et al.*, 1997] and therefore anthropogenic, and that 1/3 of the global anthropogenic aerosol is from biomass burning [IPCC, 2001], reduces the anthropogenic fraction to an average of  $0.21 \pm 0.07$ .

#### 4. Anthropogenic Forcing

[18] The global aerosol radiative effect over cloud free ocean is estimated to be [Boucher and Tanré, 2000; Bellouin *et al.*, 2003; Chou *et al.*, 2002; Yu *et al.*, 2004] in the range of  $-3.8$  to  $-6.0$   $\text{W/m}^2$ . L. A. Remer and Y. J. Kaufman (Direct aerosol radiative effect over the global oceans derived from MODIS retrievals, submitted to *Atmospheric Chemistry and Physics*, 2005) used MODIS aerosol data to retrieve the aerosol radiative effect at the top of the atmosphere over cloud free ocean as:  $F_{\text{aer}} = -5.7 \pm 0.4$   $\text{W/m}^2$ . The analysis also derives the average forcing efficiency for the different aerosol types. Forcing efficiency is defined as the radiative effect at the top of the atmosphere per unit aerosol optical thickness. For the MODIS aerosol models the forcing efficiency of the fine pollution and smoke particles is estimated to be  $20 \pm 30\%$  higher from the average aerosol forcing efficiency. The anthropogenic forcing,  $\Delta F_{\text{anth}}$ , is therefore given by the product of the ratio of the anthropogenic AOT to total, the ratio of anthropogenic aerosol forcing efficiency,  $f_{\text{ef-ant}}$ , to total,  $f_{\text{ef}}$ , and the aerosol radiative effect:

$$\begin{aligned}\Delta F_{\text{anth}} &= (\tau_{\text{anth}}/\tau)(f_{\text{ef-ant}}/f_{\text{ef}})F_{\text{aer}} \\ &= (21 \pm 7\%) * (1.2 \pm 0.3) * (-5.7 \pm 0.4 \text{ W/m}^2) \\ &= -1.4 \pm 0.4 \text{ W/m}^2\end{aligned}$$

#### 5. Summary

[19] The MODIS ability to distinguish from space between fine and coarse aerosols was used to derive the anthropogenic component of the aerosol optical thickness of 0.033 over cloud free oceans. Even though chemical transport models disagree with the MODIS measurements regarding the total aerosol optical thickness (0.14 for MODIS and  $0.090 \pm 0.005$  for the three models used here), they agree regarding the anthropogenic component within 0.003. This result shows that the combination of source strength and global distribution of the models agrees with the satellite measurements, increasing the confidence in the IPCC estimates of the aerosol direct radiative forcing, using the chemical transport models.

[20] **Acknowledgments.** Part of the work was performed while Y. J. Kaufman was a visiting professor in the Laboratory for Atmospheric Optics University of Sciences and Technologies, Lille, France. Work of Olivier Boucher at the Met Office was supported by the UK Defra Climate Prediction Programme.

#### References

Albrecht, B. A. (1989), Aerosols, cloud microphysics, and fractional cloudiness, *Science*, *245*, 1227–1230.

- Bellouin, N., O. Boucher, D. Tanré, and O. Dubovik (2003), Aerosol absorption over the clear-sky oceans deduced from POLDER-1 and AERONET observations, *Geophys. Res. Lett.*, *30*(14), 1748, doi:10.1029/2003GL017121.
- Boucher, O., and D. Tanré (2000), Estimation of the aerosol perturbation to the Earth's radiative budget over oceans using POLDER satellite aerosol retrievals, *Geophys. Res. Lett.*, *27*, 1103–1106.
- Charlson, R. J., et al. (1992), Climate forcing of anthropogenic aerosols, *Science*, *255*, 423–430.
- Chin, M., et al. (2002), Tropospheric aerosol optical thickness from the GOCART model and comparisons with satellite and Sun photometer measurements, *J. Atmos. Sci.*, *59*, 461–483.
- Chou, M.-D., P. K. Chan, and M. H. Wang (2002), Aerosol radiative forcing derived from SeaWiFS-retrieved aerosol optical properties, *J. Atmos. Sci.*, *59*, 748–757.
- Gunn, R., and B. B. Phillips (1957), An experimental investigation of the effect of air pollution on the initiation of rain, *J. Meteor.*, *14*, 272–280.
- Hobbs, P. V., et al. (1997), Direct radiative forcing by smoke from biomass burning, *Science*, *272*, 1776–1778.
- Intergovernmental Panel on Climate Change (IPCC) (2001), *Climate Change 2001: The Scientific Basis: Contribution of Working Group I to the Third Assessment Report of the Intergovernmental Panel on Climate Change*, edited by J. T. Houghton et al., 881 pp., Cambridge Univ. Press, New York.
- Kaufman, Y. J., A. Smirnov, B. N. Holben, and O. Dubovik (2001), Baseline maritime aerosol: Methodology to derive the optical thickness and scattering properties, *Geophys. Res. Lett.*, *28*, 3251–3254.
- Kaufman, Y. J., D. Tanré, and O. Boucher (2002), A satellite view of aerosols in the climate system, *Nature*, *419*, 215–223.
- Kaufman, Y. J., I. Koren, L. A. Remer, D. Tanré, P. Ginoux, and S. Fan (2005), Dust transport and deposition observed from the Terra-Moderate Resolution Imaging Spectroradiometer (MODIS) spacecraft over the Atlantic Ocean, *J. Geophys. Res.*, *110*, D10S12, doi:10.1029/2003JD004436.
- Koren, I., Y. J. Kaufman, L. A. Remer, and J. V. Martins (2004), Measurement of the effect of Amazon smoke on inhibition of cloud formation, *Science*, *303*, 1342–1344.
- Prospero, J. M., and P. J. Lamb (2003), African droughts and dust transport to the Caribbean: Climate change implications, *Science*, *302*, 1024–1027.
- Ramanathan, V., et al. (2001), Aerosols, climate, and the hydrological cycle, *Science*, *294*, 2119–2124.
- Remer, L. A., et al. (2005), The MODIS aerosol algorithm, products and validation, *J. Atmos. Sci.*, *62*, 947–973.
- Rosenfeld, D. (2000), Suppression of rain and snow by urban and industrial air pollution, *Science*, *287*, 1793–1796.
- Takemura, T., et al. (2002), Single-scattering albedo and radiative forcing of various aerosol species with a global three-dimensional model, *J. Clim.*, *15*, 333–352.
- Tanré, D., Y. J. Kaufman, M. Herman, and S. Mattoo (1997), Remote sensing of aerosol over oceans from EOS-MODIS, *J. Geophys. Res.*, *102*, 16,971–16,988.
- Tanré, D., et al. (2001), Climatology of dust aerosol size distribution and optical properties derived from remotely sensed data in the solar spectrum, *J. Geophys. Res.*, *106*, 18,205–18,217.
- Tegen, I., et al. (2004), Relative importance of climate and land use in determining present and future global soil dust emission, *Geophys. Res. Lett.*, *31*(5), L05105, doi:10.1029/2003GL019216.
- Twomey, S., M. Piepgrass, and T. L. Wolfe (1984), An assessment of the impact of pollution on the global albedo, *Tellus, Ser. B*, *36*, 356–366.
- Yu, H., et al. (2004), The direct radiative effect of aerosols as determined from a combination of MODIS and GOCART simulations, *J. Geophys. Res.*, *109*, D03206, doi:10.1029/2003JD003914.

O. Boucher, Climate, Chemistry, and Ecosystems Team, Met Office, FitzRoy Road, Exeter EX1 3PB, UK.

M. Chin, Y. J. Kaufman, and L. A. Remer, NASA Goddard Space Flight Center, code 613, Greenbelt, MD 20771, USA. (yoram.j.kaufman@nasa.gov)

T. Takemura, Research Institute for Applied Mechanics, Kyushu University, 6-1 Kasuga-koen, Kasuga, Fukuoka 816-8580, Japan.

D. Tanré, Laboratoire d'Optique Atmosphérique, CNRS, Université des Sciences et Technologies de Lille 1, F-59655 Villeneuve d'Ascq, France.